Int. J. Heat Mass Transfer. Vol. 34, No. 1, pp. 11–30, 1991
Printed in Great Britain

0017–9310/91 $3.00 + 0.00
Pergamon Press plc

Modelling of developing nearly homogeneous turbulence of velocity and scalar fields

V. U. BONDARCHUK, B. A. KOLOVANDIN and O. G. MARTYNENKO

A. V. Luikov Heat and Mass Transfer Institute of the BSSR Academy of Sciences, Minsk, 220728, U.S.S.R.

(*Received* 25 *October* 1989)

Abstract—Based on the second-order model suggested by Kolovandin and Martynenko (Heat/mass transfer in homogeneous turbulence, 9th Int. Heat Transfer Conf., Jerusalem (1990)) numerical modelling of the nearly homogeneous turbulence of the velocity and transported passive scalar fields is considered. The work is aimed at a detailed study of the effect exerted by the basic factors of turbulence generation—the gradients of the averaged velocity and scalar values—on the evolution in time of the statistical characteristics of turbulence which, within the framework of the second-order model, determine the processes of turbulent momentum and heat transfer at arbitrary turbulent Reynolds and Peclet numbers.

1. INTRODUCTION

THE PROGRESS in numerical modelling of turbulent heat or mass transfer on the basis of second-order models is much inferior to that made in velocity field simulation. This can be ascribed to a number of reasons: insufficient knowledge of the elementary events of transport realizable in kinematically simple forms of a turbulent scalar field, scarce experimental data on the dynamics of the statistical parameters of turbulent transport (the variance and fluxes of the scalar, the rate of 'smearing' of scalar fluctuations) in a developing turbulence at arbitrary turbulent Reynolds and Peclet numbers, etc. It is not improbable that some of these reasons could be obviated by direct modelling of turbulent transfer based on the numerical solution of three-dimensional non-stationary Navier–Stokes and transport equations should there have also been a priori confidence that the numerical time realization of a respective function at the given point of space adequately fitted the real physical process. Such an adequacy could be successfully checked by second-order models involving exact asymptotic solutions that could be obtained with the alternative, say spectral, technique. In other words, there should exist a feedback between the method of direct numerical simulation and modelling based on 'adequate' second-order models which could make it possible to perfect both approaches aimed ultimately at the solution of the practical problems of turbulent transfer.

The present paper deals with the solution of 'test' problems concerning the dynamics of the nearly homogeneous turbulence of velocity and scalar fields on the basis of the second-order model suggested in ref. [1]. The nearly homogeneous turbulence here is meant to be such which is generated by constant, transverse to the motion of fluid, gradients of the mean values of velocity and transported scalar. The reference to this kind of turbulence is due, on the one hand, to its relative simplicity (no factor of turbulent diffusion in model equations) allowing comparison with the data on direct numerical simulation and, on the other hand, to its realistic approximation to the shear flow turbulence.

2. THE DYNAMICS OF A NEARLY HOMOGENEOUS VELOCITY FIELD

The second-order model of a nearly homogeneous turbulent velocity field consists of a model differential equation for the Reynolds stress tensor

$$\frac{\mathrm{D}}{\mathrm{D}\tau}\overline{u_iu_j} - P_{ij} + 2\left[d_u\frac{\overline{u_iu_j}}{\overline{q^2}} + (1-d_u)\frac{1}{3}\delta_{ij}\right]\varepsilon_u + a_u(1-d_u)a_{ij}\varepsilon_u + b_u[\alpha_u\overline{q^2}S_{ij} + (\beta_u b_{ij} + \gamma_u c_{ij})P_{kk}] = 0 \quad (1)$$

and an equation for the turbulent kinetic energy dissipation rate

$$\frac{\mathrm{D}}{\mathrm{D}\tau}\varepsilon_u + (\mathscr{F}_u^{**} - 3\bar{P}_u)\frac{\varepsilon_u^2}{q^2} = 0 \quad (2)$$

where $\overline{q^2} = \overline{u_i^2}$ is the doubled kinetic energy turbulence

$$P_{ij} = -\left(\overline{u_iu_k}\frac{\mathrm{d}U_j}{\mathrm{d}x_k} + \overline{u_ju_k}\frac{\mathrm{d}U_i}{\mathrm{d}x_k}\right)$$

is the second-rank tensor of the rate of Reynolds stress generation due to the mean shear (in the present case of nearly homogeneous turbulence $\partial U_i/\partial x_l = \mathrm{d}U_1/\mathrm{d}x_2 = \text{const.}$)

$$a_{ij} = 3\overline{u_iu_j}/\overline{q^2} - \delta_{ij}$$

is the deviator of the Reynolds stress tensor

$$S_{ij} = \frac{1}{2}\left(\frac{\partial U_i}{\partial x_j} + \frac{\partial U_j}{\partial x_i}\right)$$

NOMENCLATURE

F_{t1}, F_{t2} interaction functions in equation for ε_t
F_u interaction function in equation for ε_u
L_t Taylor macroscale of scalar field, $6(\overline{q^2})^{1/2}\overline{t^2}/\varepsilon_t$
P_λ turbulent Peclet number, $(\overline{q^2})^{1/2}\lambda_t/\kappa$
R time scale ratio, τ_u/τ_t
R_{awo} time scale ratio in the final stage of decay of nearly homogeneous scalar field in isotropic velocity field
R_λ turbulent Reynolds number, $(\overline{q^2})^{1/2}\lambda_u/\nu$
$\overline{q^2}$ doubled kinetic energy of turbulence, $\overline{u_i^2}$
T mean value of a scalar
t pulsation of a scalar
$\overline{t^2}$ scalar variance
u_i vector of velocity fluctuations
$\overline{u_i t}$ vector of turbulent flux
$\overline{u_i u_j}$ second-rank tensor of Reynolds stresses
U_i vector of mean velocity
x_i Cartesian coordinate ($i = 1, 2, 3$)
x_1 longitudinal coordinate
x_2 transverse coordinate.

Greek symbols

ε_t rate of scalar variance smearing
ε_u rate of kinetic energy of turbulence dissipation
λ_t^2 squared Taylor microscale of scalar field, $\sigma\kappa\overline{t^2}/\varepsilon_t$
λ_u^2 squared Taylor microscale of velocity field, $5\nu q^2/\varepsilon_u$
ν kinematic viscosity
κ molecular diffusivity
σ molecular Prandtl number, ν/κ
σ_{Tawo} asymptotic value of the turbulent Prandtl number in the final stage of degeneration of a nearly homogeneous scalar field in an isotropic velocity field
τ time
τ_t scalar time scale, t^2/ε_t
τ_u velocity time scale, q^2/ε_u.

Subscripts

i, j, k tensor indices
o absence of mean scalar
s strong turbulence, $R_\lambda \gg 1$
T large-scale eddy
t scalar
w weak turbulence, $R_\lambda \ll 1$.

Superscripts

$\overline{\ }$ averaging operation
o virtual origin
* homogeneity
** isotropy.

is the tensor of mean shear

$$b_{ij} = 3P_{ij}/P_{kk} - \delta_{ij}$$

is the deviator of the tensor P_{ij}

$$c_{ij} = 3D_{ij}/P_{kk} - \delta_{ij}$$

is the deviator of the tensor D_{ij}

$$D_{ij} = -\left(\overline{u_i u_k}\frac{\partial U_k}{\partial x_j} + \overline{u_j u_k}\frac{\partial U_k}{\partial x_i}\right)$$

$$\bar{P}_u = P_{kk}/2\varepsilon_u$$

is the ratio of the turbulent kinetic energy generation to the rate of its dissipation

$$\mathscr{F}_u^{**}(R_\lambda) = \frac{11}{3}(1-d_u) + \frac{14}{5}d_u = \frac{11}{3} - \frac{13}{15}d_u$$

is the interaction function of turbulent vortices of different scales

$$d_u = 1 - 2/(1+\sqrt{(1+\delta_u/R_\lambda^2)})$$

where

$$R_\lambda^2 = \frac{5}{\nu}\frac{(\overline{q^2})^2}{\varepsilon_u}$$

is the squared turbulent Reynolds number

$$b_u = 2\{1 + [(\alpha_s/(\mathscr{F}_{us}^{**} - 2))(1-d_u) + (\alpha_w/(\mathscr{F}_{uw} - 2))d_u]\bar{P}_u\}^{-1}$$

$$\alpha_u = 2\left(\frac{1}{11}d_u - \frac{1}{10}\right), \quad \beta_u = \frac{4}{33}d_u, \quad \gamma_u = -\frac{1}{33}d_u$$

$$a_u \simeq 3, \quad \delta_u \simeq 2800, \quad \mathscr{F}_{us}^{**} = 11/3, \quad \mathscr{F}_{uw}^{**} = 14/5$$

$$\alpha_s \simeq 1, \quad \alpha_w \simeq 0.5.$$

With some assumptions, the above model may yield exact asymptotic solutions for the dynamics of a nearly homogeneous turbulence.

2.1. *The dynamics of a strong ($R_\lambda \gg 1$) nearly homogeneous velocity field*

Consider turbulence evolving in time and being generated by a constant, transverse to the fluid motion, mean-velocity gradient $dU_1/dx_2 = \text{const}$.

On the assumption of equilibrium of large vortices [1], i.e. at

$$\frac{\tau_U}{\tau_u} = \frac{\nu_T/\overline{q^2}}{\overline{q^2}/\varepsilon_u} = \frac{(-\overline{u_1 u_2}/(dU_1/dx_2))/\overline{q^2}}{\overline{q^2}/\varepsilon_u} = n_u = \text{const.} \tag{3}$$

equations (1) and (2) take on the form

$$\frac{\mathrm{D}}{\mathrm{D}\tau}\overline{q^2} = 2(n_{us}\bar{\tau}_u^2 - 1)\overline{q^2}/\bar{\tau}_u$$

$$\frac{\mathrm{D}}{\mathrm{D}\tau}\bar{\tau}_u = \mathscr{F}_{us}^{**} - 2 - n_{us}\bar{\tau}_u^2 \qquad (4)$$

where $\bar{\tau}_u = \tau_u \, \mathrm{d}U_1/\mathrm{d}x_2$ and the subscript 's' denotes a strong turbulence.

It can be shown that the asymptotic (for $\bar{\tau} \gg 1$) solution to system (4) has the form

$$\overline{q^2} = \overline{q_{\mathrm{ref}}^2} \exp\left[2\frac{\bar{P}_u - 1}{\bar{P}_u}\left(-\frac{\overline{u_1u_2}}{\overline{q^2}}\right)(\bar{\tau} - \bar{\tau}_{\mathrm{ref}})\right]$$

$$\bar{\tau}_u^2 = \frac{1}{n_{us}}(\mathscr{F}_{us}^{**} - 2) = \frac{5}{3}\frac{1}{n_{us}} \qquad (5)$$

where $\overline{q_{\mathrm{ref}}^2}$ is a fixed value of $\overline{q^2}$.

The remaining characteristics of turbulence can be represented as

$$\bar{P}_u = (\mathscr{F}_{us}^{**} - 2) = \frac{5}{3}$$

$$\left(-\frac{\overline{u_1u_2}}{\overline{q^2}}\right)^2 = (n_{us}\bar{\tau}_u)^2 = n_{us}(\mathscr{F}_{us}^{**} - 2) = \frac{5}{3}n_{us}$$

$$\overline{u_1^2}/\overline{q^2} \simeq 0.55, \quad \overline{u_2^2}/\overline{q^2} \simeq 0.23 \qquad (6)$$

where $n_{us} \simeq 1.5 \times 10^{-2}$ is an empirical factor taken into account in the relation for b_{us}.

Thus, the evolution in time of a strong nearly homogeneous turbulence for $\bar{\tau} \gg 1$ is characterized by an exponential growth of kinetic energy and by the asymptotic values of the parameters $\bar{P}_u$, $\bar{\tau}_u$ and $(-\overline{u_1u_2}/\overline{q^2})$. According to solution (5), in this case the turbulent Reynolds number

$$R_\lambda^2 = \frac{\overline{q^2}\lambda_u^2}{\nu^2} = \frac{5}{\nu}\frac{(\overline{q^2})^2}{\varepsilon_u} = \frac{5}{\nu}\frac{1}{\mathrm{d}U_1/\mathrm{d}x_2}\bar{\tau}_u\overline{q^2}$$

is also an increasing function of $\bar{\tau}$. Thus, the transition of the initially strong developing nearly homogeneous turbulence to the final stage is impossible.

To check the validity of solutions (5) and (6), the Cauchy problem was solved numerically at the initial values of turbulence parameters corresponding to the experiments of Champagne *et al.* [2], Harris *et al.* [3], Tavoularis and Corrsin [4], and Karnik and Tavoularis [5]. The results of numerical modelling are presented in Figs. 1–4. It is seen from Fig. 1 that, depending on the initial conditions, at the start of evolution, the kinetic energy of turbulence

$$E = \overline{q^2}h^2/(\mathrm{d}U_1/\mathrm{d}x_2)^2$$

where h is the lateral dimension of a channel, can be a decreasing function of time

$$\bar{\tau} = \tau\frac{\mathrm{d}U_1}{\mathrm{d}x_2} = \frac{x_1}{h}\left(\frac{h}{U_c}\mathrm{d}U_1/\mathrm{d}x_2\right)$$

where U_c is the centreline velocity. Such a situation is realizable at the initial values of the shear parameter $\bar{P}_u$ smaller than unity. At large values of $\bar{\tau}$, the function E approaches the exponential asymptotics (5) attained only in some of the experiments considered.

As presented in Fig. 2, the evolution of the velocity time scale $\bar{\tau}_u = (\overline{q^2}/\varepsilon_u)\,\mathrm{d}U_1/\mathrm{d}x_2$ related to the Taylor microscale of length $\lambda_u^2 = 5\nu\overline{q^2}/\varepsilon_u$ by the relation $\bar{\tau}_u = \frac{1}{5}R_c(\lambda_u/h)^2$, where $R_c = (\mathrm{d}U_1/\mathrm{d}x_2)h^2/\nu$ is the mean gradient-based Reynolds number, shows that with $\bar{\tau} \gg 1$ the parameter $\bar{\tau}_u$ tends to the constant universal value indicated in solution (5). Unfortunately, the lack of experimental data does not allow one to judge the adequacy of the modelling of this parameter. Nevertheless, it can be said that the individual data of refs. [2, 3] fit the numerical curves, whereas the data of ref. [4] differ significantly from numerical results. Here, it should be borne in mind that the rate of dissipation is measured not directly but with resorting to the hypothesis of local isotropy thus allowing the occurrence of considerable errors in such a sub-

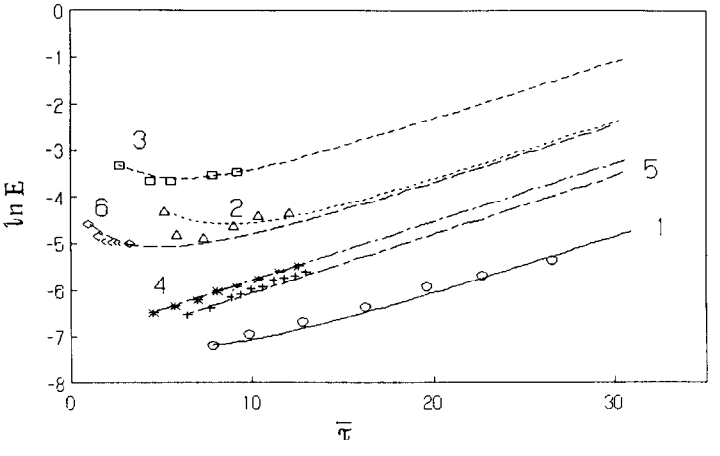

FIG. 1. Evolution of the kinetic energy of nearly homogeneous strong turbulence: ○, undisturbed flow; △, $M = 2.5$; □, $M = 5$ [5]; *, ref. [4]; +, ref. [3]; ◇, ref. [2]; ——, numerical modelling.

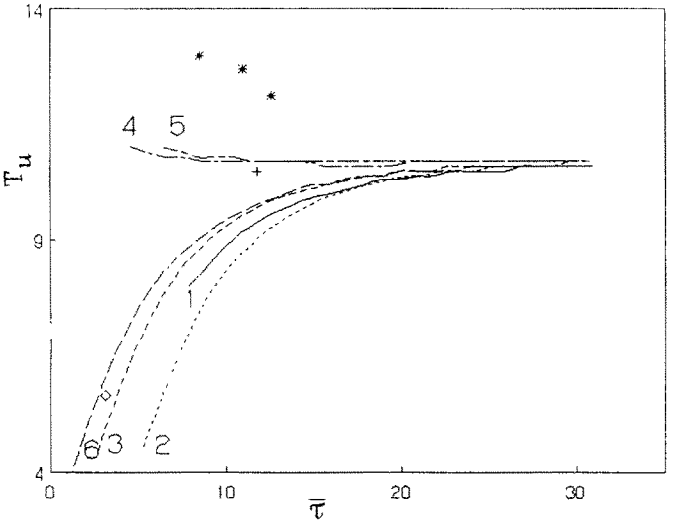

FIG. 2. Evolution of velocity time scale. For notation see Fig. 1.

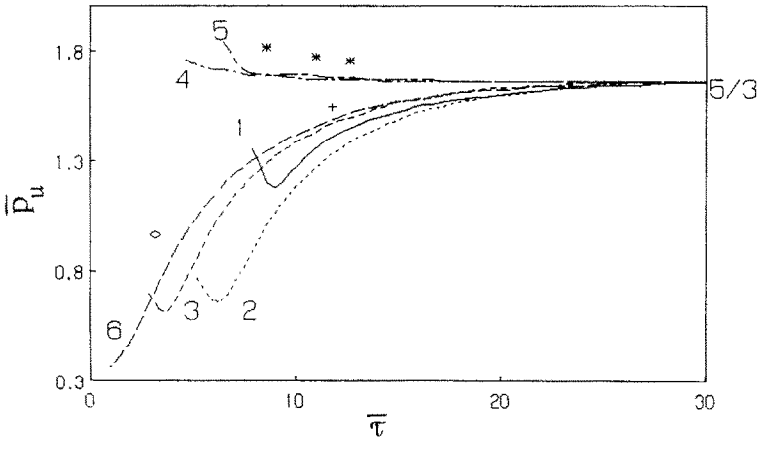

FIG. 3. Evolution of the ratio of the rate of turbulence energy generation to that of dissipation. For notation see Fig. 1.

stantially anisotropic field as is the nearly homogeneous turbulence being investigated.

The evolution of the shear parameter $\bar{P}_u = -\overline{u_1 u_2} \times (\mathrm{d}U_1/\mathrm{d}x_2)/\varepsilon_u$ presented in Fig. 3, shows that at large values of $\bar{\tau}$ this parameter also tends to the universal constant value indicated in solution (6). As regards the comparison between the predicted and experimental data, the same conclusion can be made as that for the previous function $\bar{\tau}_u$ (or λ_u^2).

As presented in Fig. 4, the evolution of normal and tangential Reynolds stresses related to the kinetic energy of turbulence, i.e. of the parameters $K_{11} = (\overline{u_1^2}/\overline{q^2})$, $K_{22} = (\overline{u_2^2}/\overline{q^2})$, $K_{12} = -(\overline{u_1 u_2}/\overline{q^2})$, shows the validity of asymptotic relations (6); as regards the empirical data, the indicated asymptotic was attained only in one realization of Karnik and Tavoularis' experiment in which the shear was produced by a multi-layered fluid flow without a turbulizor.

All the experiments indicated above were carried out for large initial turbulent Reynolds numbers that prevented the possibility of transition to a weak turbulence.

2.2. *The dynamics of a weak* ($R_\lambda \ll 1$) *nearly homogeneous velocity field*

On the condition that at the start of evolution the turbulence, generated by the lateral velocity gradient, is weak and with assumption (3), the system of equations (1) and (2) admits an asymptotic (for $\bar{\tau} \gg 1$) solution such as (5) where the coefficient F_{us}^{**} is substituted by the coefficient $F_{uw}^{**} = 14/5$ and n_{us} by

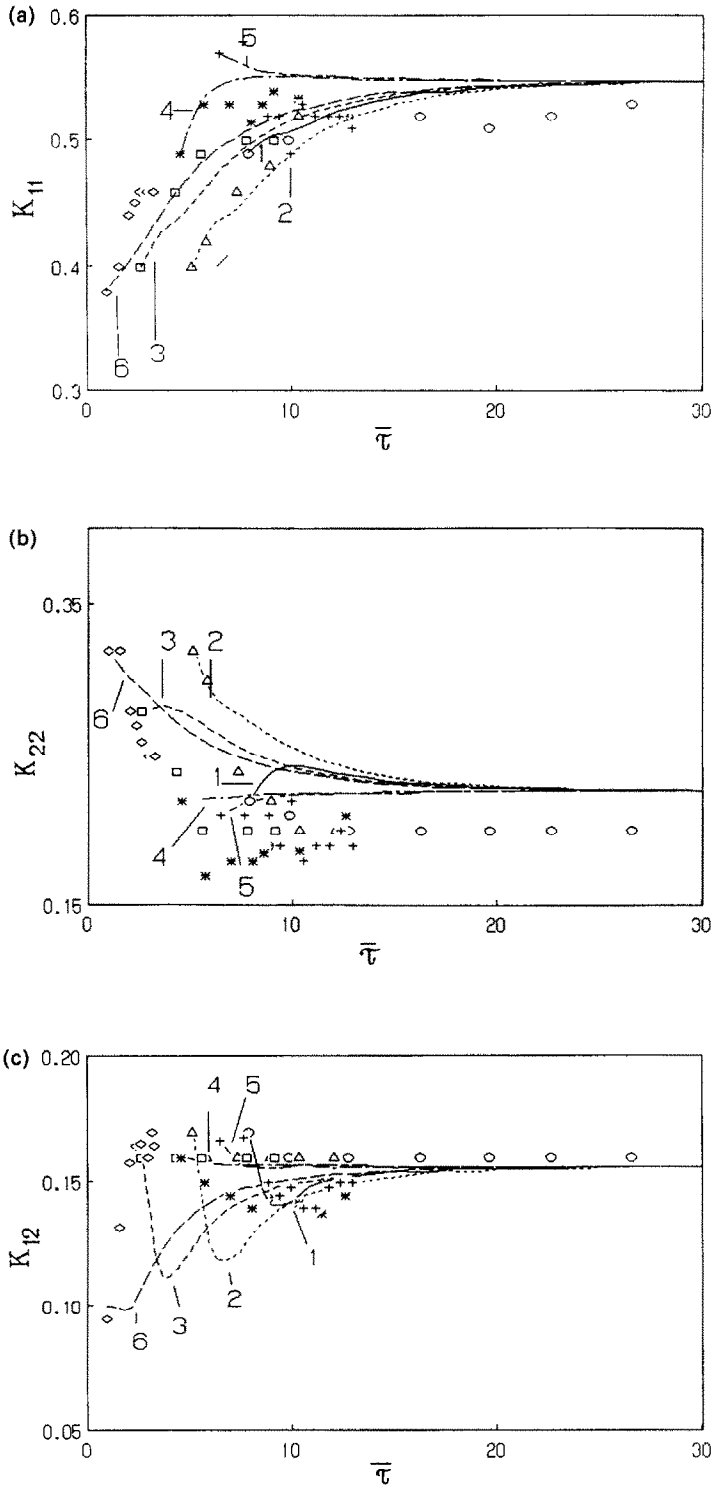

FIG. 4. Evolution of the ratios of Reynolds stresses to kinetic energy: (a) k_{11}; (b) k_{22}; (c) k_{12}. Notation as in Fig. 1.

$n_{uw} \simeq 1.25 \times 10^{-3}$, i.e.

$$q^2 = q_{ref}^2 \exp\left[2\frac{\bar{P}_u - 1}{\bar{P}_u}\left(-\frac{u_1u_2}{q^2}\right)\bar{\tau}\right]$$

$$\bar{\tau}_u = \frac{1}{n_{uw}}(\mathscr{F}_{uw}^{**} - 2)$$

$$\bar{P}_u = (\mathscr{F}_{uw}^{**} - 2)$$

$$\left(-\frac{\overline{u_1u_2}}{\overline{q^2}}\right)^2 = n_{uw}(\mathscr{F}_{uw}^{**} - 2) \quad (7)$$

$$\overline{u_1^2}/\overline{q^2} \simeq 0.62, \quad \overline{u_2^2}/\overline{q^2} \simeq 0.25, \quad \overline{u_3^2}/\overline{q^2} \simeq 0.13. \quad (8)$$

The fundamental difference of solution (7) for $\overline{q^2}$ when $R_\lambda \ll 1$ from solution (5) consists of the fact that in the case of the weak turbulence considered the exponent is the negative quantity the value of which is dictated by the coefficients F_{uw}^{**} and n_{uw}. Thus, in weak nearly homogeneous turbulence $\overline{q^2}$ is a decreasing function of time.

Unfortunately, experimental realization of the mode of a weak nearly homogeneous turbulence is unknown to date. Such a situation was the object of theoretical studies by Deissler [6] (which provided the assessing value for the above given coefficient n_{uw}). Comparison of the aforegoing asymptotic solutions with the results of Deissler's analysis shows that the data for $\overline{q^2}$ and $\overline{u_1u_2}$ agree, whereas relations (8) for normal stresses are inconsistent with Deissler's data according to which $(\overline{u_i^2}/\overline{q^2}) \to 0$ when $\bar{\tau} \gg 1$.

2.3. *The dynamics of a nearly homogeneous velocity field at arbitrary R_λ values*

As indicated above, at large initial values of the parameter R_λ the transition of homogeneous turbulence to the final stage is impossible. At the same time, the feasibility of an asymptotically weak turbulence in principle, relations (7) and (8), raises the question whether or not the transition to the final stage is possible at moderate initial values of R_λ. To resolve this question, a conventional numerical experiment was carried out with the system of equations (1) and (2) at the given initial values for the variables corresponding to ref. [4] and at different initial turbulent Reynolds numbers

$$R_\lambda^2 = 5R_cE\bar{\tau}_u.$$

The results of numerical simulation of the nearly homogeneous turbulence evolution are presented in Figs. 5–8 for $R_c^o = 150$, i.e. at $R_\lambda^o = 4.6$. As is seen from Fig. 5, at the start of evolution the parameters E and R_λ increase just as in the case of a strong turbulence. When R_λ attains the value approximately equal to 6.5, there appears a characteristic intermediate stretch over which all of the parameters vary slowly (see Figs. 6–8). Beginning from $R_\lambda \simeq 6$ a rapid transition is observed to the final stage which commences at $R_\lambda \simeq 0.1$. At great values of $\bar{\tau}$ the numerical solution approaches the asymptotics of the final stage, relations (7) and (8).

Thus, the transition of the evolving nearly homogeneous turbulence to the final stage of decay is feasible at moderate initial values of the turbulent Reynolds number not exceeding $R_\lambda \simeq 6.5$.

3. THE DYNAMICS OF A NEARLY HOMOGENEOUS SCALAR FIELD

The second-order model of a nearly homogeneous scalar field [1] consists of a model differential equation

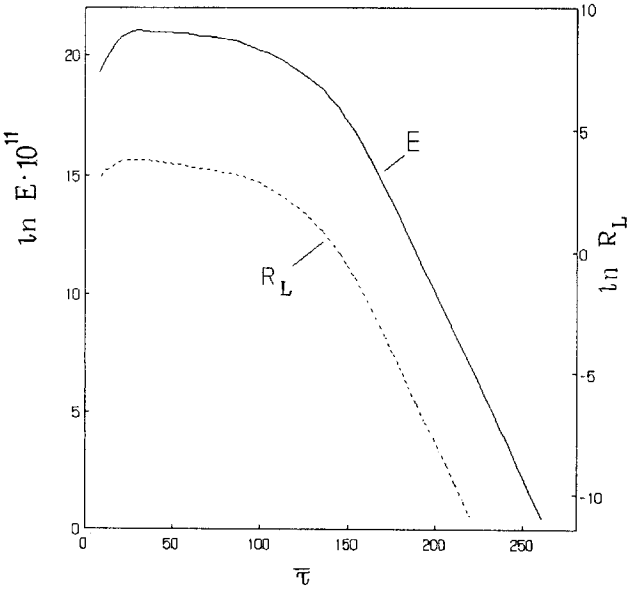

FIG. 5. Evolution of kinetic energy and turbulent Reynolds number $R_L = R_\lambda^2$ up to the final stage of degeneration.

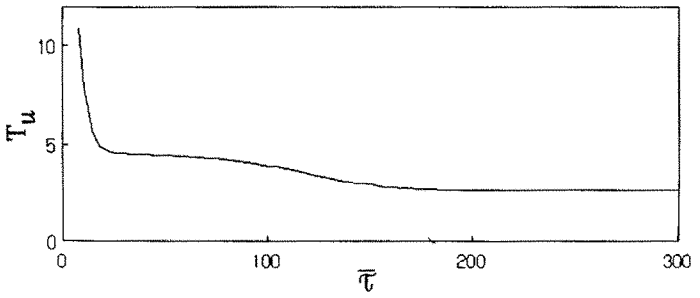

FIG. 6. Evolution of velocity time scale T_u.

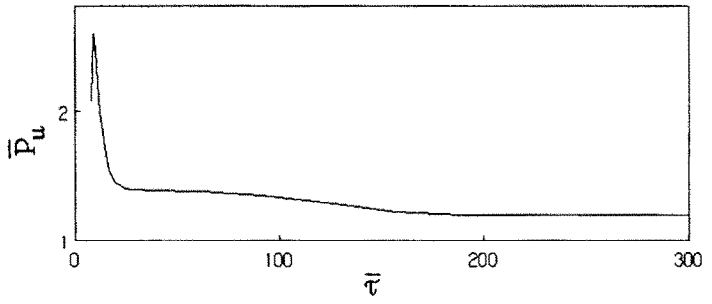

FIG. 7. Evolution of the parameter $\bar{P}_u$.

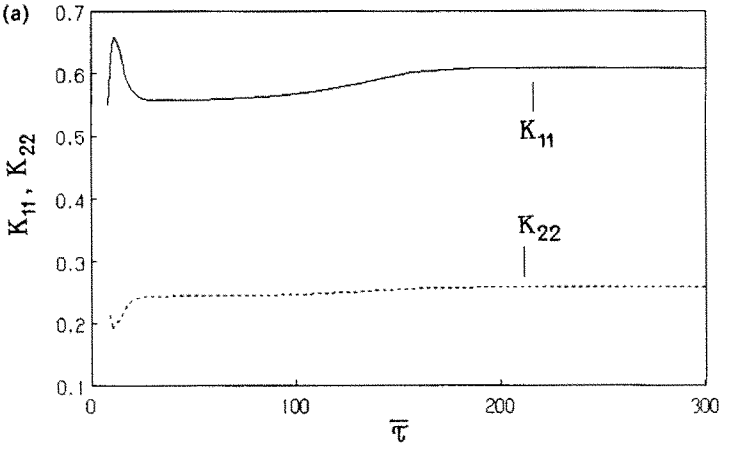

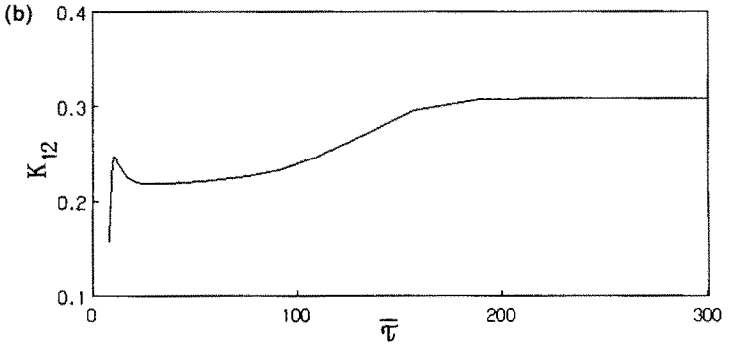

FIG. 8. Evolution of Reynolds stresses: (a) k_{11}, k_{22}; (b) k_{12}.

for the turbulent flux vector

$$\frac{\mathrm{D}}{\mathrm{D}\tau}\overline{u_i t} - P_{it} + \frac{1}{\tau_{ut}}\overline{u_i t} = 0 \tag{9}$$

and exact equation for the mean squared fluctuations of a scalar

$$\frac{\mathrm{D}}{\mathrm{D}\tau}\overline{t^2} + 2(1-\bar{P}_t)\varepsilon_t = 0 \tag{10}$$

and of a model equation for the rate of 'smearing' of scalar fluctuations

$$\frac{\mathrm{D}}{\mathrm{D}\tau}\varepsilon_t - d_u\left(2\bar{P}_u\varepsilon_u/\overline{q^2} + \frac{2\bar{P}_t}{1+\sigma}\frac{1}{\tau_{utw}}\right)\varepsilon_t + (\mathscr{F}_{t1}^{*}\varepsilon_u/\overline{q^2} + \mathscr{F}_{t2}^{*}\varepsilon_t/\overline{t^2})\varepsilon_t = 0 \tag{11}$$

where

$$P_{it} = -\left(\overline{u_i u_k}\frac{\partial T}{\partial x_k} + \overline{u_k t}\frac{\partial U_i}{\partial x_k}\right)$$

is the vector of the flux generation rate due to the mean lateral shear and to the transverse gradient of the mean value of the scalar

$$\frac{1}{\tau_{ut}} = (1-d_u)\frac{1}{\tau_{uts}} + d_u\frac{1}{\tau_{utw}}$$

is the quantity reciprocal of the mixed time scale

$$\frac{1}{\tau_{uts}} = \left[(4-\mathscr{F}_{us}^{**}) + \frac{1}{n_{ts}}(\overline{u_2^2}/\overline{q^2})R - \bar{P}_u\right]\varepsilon_u/\overline{q^2}$$

$$\frac{1}{\tau_{utw}} = \left\{\left(1-\frac{2\bar{P}_t}{1+\sigma}\right)^{-1}[f_3-(f_1-1)\bar{P}_u] + f_2 R\right\}\varepsilon_u/\overline{q^2}$$

$$\mathscr{F}_{t1}^{*} = \mathscr{F}_{t1}^{**} - \bar{P}_u + d_u f_1 \bar{P}_u$$

$$\mathscr{F}_{t2}^{*} = \mathscr{F}_{t2}^{**} - 2\bar{P}_t + d_u\left(\frac{2\bar{P}_t}{1+\sigma}\right)f_2$$

$$\mathscr{F}_{t1}^{**} = \mathscr{F}_{u}^{**} - 2 + \frac{4}{5}d_u, \quad \mathscr{F}_{t2}^{**} = 2 + \frac{4}{3}d_u$$

$$f_1 = \left(1-\frac{2\bar{P}_t}{1+\sigma}\right) + 1$$

$$f_2 = \left[2\left(\sigma_{\mathrm{Tawo}} + \frac{3}{5}\right) - \frac{4}{3}\left(R_{\mathrm{awo}} - \frac{3}{5}\right)\frac{1+\sigma}{2\bar{P}_t}\right]\frac{1}{R_{\mathrm{awo}}}$$

$$f_3 = \frac{4}{3}\left(\left(1-\frac{2\bar{P}_t}{1+\sigma}\right)\Big/\frac{2\bar{P}_t}{1+\sigma}\right)\left(R_{\mathrm{awo}} - \frac{3}{5}\right)\frac{R}{R_{\mathrm{awo}}}$$

where

$$R_{\mathrm{awo}} = \frac{1}{5\sigma}\left[1-2\left(\frac{2\sigma}{1+\sigma}\right)^{3/2} + \sigma^{3/2}\right]\Big/\left[1-2\left(\frac{2\sigma}{1+\sigma}\right)^{1/2} + \sigma^{1/2}\right]$$

is the parameter of the scale ratio in the final stage of degeneration of the nearly homogeneous scalar field in the isotropic velocity field [7]

$$\sigma_{\mathrm{Tawo}} = \frac{3}{10}\frac{1-\sigma}{\sigma}\Big/\left[1-\left(\frac{2\sigma}{1+\sigma}\right)^{1/2}\right]$$

is the turbulent Prandtl number in the final stage of degeneration of the nearly homogeneous scalar field in the isotropic velocity field, $\sigma = \nu/\kappa$ is the molecular Prandtl number

$$\frac{1}{n_{ts}} = \frac{1}{n_{tso}}[1+3\bar{P}_u/(\mathscr{F}_{us}^{**}-2)], \quad n_{tso} \simeq 10^{-1}.$$

The above second-order model of a nearly homogeneous scalar field envisages any means of the scalar field generation with any way of velocity field generation. In the simplest case, a homogeneous isotropic degenerating velocity field transports a homogeneous isotropic degenerating scalar field. In this case, the asymptotic (for $R_\lambda \gg 1$, $P_\lambda \gg 1$) solution for the evolution of the velocity and passive scalar fields can be presented [8] in the form of power 'laws':

$$\overline{q^2} = (\overline{q^2})^{\circ}(\tau^{\circ})^{2/(\mathscr{F}_{us}^{**}-2)}(\tau+\tau^{\circ})^{-2/(\mathscr{F}_{us}^{**}-2)}$$

$$\tau_u = (\mathscr{F}_{us}^{**}-2)(\tau+\tau^{\circ})$$

$$\overline{t^2} = (\overline{t^2})^{\circ}(\tau^{\circ})^{2R^{\circ}/(\mathscr{F}_{us}^{**}-2)}(\tau+\tau^{\circ})^{-2R^{\circ}/(\mathscr{F}_{us}^{**}-2)}$$

$$\tau_t = (\mathscr{F}_{us}^{**}-2)(\tau+\tau^{\circ})/R^{\circ}$$

$$\overline{t^2}L_t^{3R^{\circ}} = \text{const.}, \quad R = R^{\circ} = \text{const.} \tag{12}$$

where

$$\tau^{\circ} = -\frac{1}{\mathscr{F}_{us}^{**}-2}\frac{(\overline{q^2})^{\circ}}{\varepsilon_u^{\circ}} = \frac{\tau_u^{\circ}}{\mathscr{F}_{us}^{**}-2}$$

is the virtual origin.

When $R_\lambda \ll 1$, $P_\lambda \ll 1$, the system of isotropic equations has the well-known Loitsyanskiy–Corrsin solution.

In a more complex case of $\bar{P}_u = 0$ and $\bar{P}_t \neq 0$ the velocity field is degenerating isotropic, whereas the field of a transported scalar is the simplest nearly homogeneous one. Finally, at $\bar{P}_u \neq 0$ and $\bar{P}_t \neq 0$ the velocity and scalar fields are nearly homogeneous in the general sense.

To qualitatively analyse the evolution of a nearly homogeneous scalar field, introduce the asymptotic (for $R_\lambda \gg 1$, $P_\lambda \gg 1$ and $R_\lambda \ll 1$, $P_\lambda \ll 1$) hypothesis concerning the equilibrium of large scalar 'vortices' [1] which is analogous to hypothesis (3)

$$\frac{\tau_{\mathrm{T}}}{\tau_t} = \frac{\kappa_{\mathrm{T}}/q^2}{\overline{t^2}/\varepsilon_t} = \frac{(-\overline{u_2 t}/(\mathrm{d}T/\mathrm{d}x_2))/\overline{q^2}}{\overline{t^2}/\varepsilon_t} = n_t = \text{const.} \tag{13}$$

presumably valid both at $\bar{P}_u = 0$ and at $\bar{P}_u \neq 0$. It can be shown with the aid of this hypothesis that the equation for $\tau_t = \overline{t^2}/\varepsilon_t$ acquires the form of equation (4) for τ_u, i.e. in the evolving ultimately strong or ultimately weak nearly homogeneous velocity field the following condition holds:

$$R = \tau_u/\tau_t = \text{const.} \tag{14}$$

3.1. *Evolution of a nearly homogeneous scalar field in a decaying isotropic velocity field*

Consider the evolution of a scalar field generated by a constant transverse mean scalar gradient in a decaying isotropic velocity field in two limiting cases: strong turbulence, i.e. when $R_\lambda \gg 1$, $P_\lambda \gg 1$, and weak turbulence, i.e. when $R_\lambda \ll 1$, $P_\lambda \ll 1$.

In the case of strong turbulence, the velocity field is determined by solution (12) for $\overline{q^2}$ and τ_u. With the use of hypothesis (13), i.e. at

$$\bar{P}_t = n_{t\mathrm{so}} \left(\frac{\mathrm{d}T}{\mathrm{d}x_2}\right)^2 \tau_t^2 \overline{q^2}/\overline{t^2} \tag{15}$$

where the subscript 'o' denotes $\bar{P}_u = 0$, it can be shown that the solution of equation (10) for $\overline{t^2}$ has the form

$$\overline{t^2} = [(\overline{t^2})^\circ - (\vartheta^2)^\circ](\bar{\tau}+1)^{-2R/(\mathscr{F}_{us}^{**}-2)} + (\vartheta^2)^\circ(\bar{\tau}+1)^{2/(\mathscr{F}_{us}^{**}-3)/(\mathscr{F}_{us}^{**}-2)} \tag{16}$$

where

$$(\vartheta^2)^\circ = n_{t\mathrm{so}} \frac{(\mathscr{F}_{us}^{**}-2)}{R} \frac{1}{(\mathscr{F}_{us}^{**}-3+R)} \times \left(\frac{\mathrm{d}T}{\mathrm{d}x_2}\right)^2 (\overline{q^2})^\circ(\tau^\circ)^2$$

$$\bar{\tau} = \tau/\tau^\circ.$$

If the initial conditions are such that $(\vartheta^2)^\circ \ll (\overline{t^2})^\circ$, then relation (16) goes over into isotropic solution (12). For $\bar{\tau} \gg 1$ this relation acquires the form

$$\overline{t^2}_{/\bar{\tau}\gg 1} = (\vartheta^2)^\circ(\tau^*)^{2(\mathscr{F}_{us}^{**}-3)/(\mathscr{F}_{us}^{**}-2)} = (\vartheta^2)^\circ(\bar{\tau})^{4/5}. \tag{17}$$

This is an asymptotic (for $\bar{\tau} \gg 1$) solution for the evolution of $\overline{t^2}$ when $\bar{P}_u = 0$, $R_\lambda \gg 1$, and $P_\lambda \gg 1$. With the use of this solution, relation (15) takes on the form

$$\bar{P}_{t_{/\bar{\tau}\gg 1}} = 1 + \frac{(\mathscr{F}_{us}^{**}-2)}{R^\circ} \tag{18}$$

which indicates that at large times of the evolution of a strong nearly homogeneous scalar field in a strong degenerating velocity field an equilibrium is attained between the generation and 'dissipation' of scalar fluctuations. In this case also attained is the asymptotic value for the correlation coefficient

$$\rho_{2t}^2 = \tfrac{1}{3} n_{t\mathrm{so}} \bar{P}_t. \tag{19}$$

In the limit case of a weak turbulence, i.e. when $R_\lambda \ll 1$ and $P_\lambda \ll 1$, the velocity field is also described by relations (12) for $\overline{q^2}$ and τ_u, where $\tau \gg \tau^\circ$, whereas the parameter $\mathscr{F}_{us}^{**}$ is substituted by the parameter $\mathscr{F}_{uw}^{**} = 14/5$. With the use of hypothesis (15), i.e. at

$$\bar{P}_t = n_{t\mathrm{wo}} \left(\frac{\mathrm{d}T}{\mathrm{d}x_2}\right)^2 \tau_t^2 \overline{q^2}/\overline{t^2}$$

the asymptotic solution of differential equation (10) for $\overline{t^2}$ has the form

$$\overline{t^2}_{/\bar{\tau}\gg 1} = n_{t\mathrm{wo}} \frac{(\mathscr{F}_{uw}^{**}-2)}{R_{\alpha\mathrm{wo}}} \frac{1}{(\mathscr{F}_{uw}^{**}-3+R_{\alpha\mathrm{wo}})} \left(\frac{\mathrm{d}T}{\mathrm{d}x_2}\right)^2 \times (\overline{q^2})^\circ(\tau^\circ)^2(\bar{\tau})^{2(\mathscr{F}_{uw}^{**}-3)/(\mathscr{F}_{uw}^{**}-2)} \sim (\bar{\tau})^{-1/2} \tag{20}$$

which is coincident with the form of Dun and Reid's analytical solution [7]. With this solution taken into account, the asymptotic relation for the parameter $\bar{P}_t$ can be presented as

$$\bar{P}_{t_{/\bar{\tau}\gg 1}} = 1 - (3 - \mathscr{F}_{uw}^{**})/R_{\alpha\mathrm{wo}} \tag{21}$$

and the correlation coefficient can be given in the form

$$\rho_{2t_{/\bar{\tau}\gg 1}}^2 = \frac{1}{3}\left[1 - \left(\frac{2\sigma}{1+\sigma}\right)^{3/2}\right]^2 \Bigg/ \left[1 - 2\left(\frac{2\sigma}{1+\sigma}\right)^{1/2} + \sigma^{1/2}\right] \tag{22}$$

also following from Dun and Reid's solution.

To check the validity of asymptotic solutions (17)–(19) for $R_\lambda \gg 1$, $P_\lambda \gg 1$ and the adequacy of model (9)–(11) at arbitrary turbulent Reynolds and Peclet numbers, the Cauchy problem was solved numerically for the system of differential equations (1), (2) and (9)–(11) for $\bar{P}_u = 0$ under the initial conditions corresponding to the experiment of Sirivat and Warhaft [9].

Figures 9 and 10 present numerical and experimental results for the evolution of the velocity field parameters $E = \overline{q^2}/U_\infty^2$ and $T_u = (\overline{q^2}/\varepsilon_u)U_\infty/M$, where U_∞ is the flow velocity, M the dimension of a grid cell. In accordance with the experiment, two realizations of the nearly homogeneous scalar field were fulfilled against the background of an almost isotropic degenerating velocity field by means of a heated grid ('mandoline') and a heated honeycomb ('toaster').

Comparison of the numerical and experimental results on the evolution of the scalar field parameters in the 'mandoline' wake is presented in Figs. 11–14 for two different values of $\mathrm{d}T/\mathrm{d}x_2$. As follows from Fig. 11, which demonstrates the development of parameter $\theta = \overline{t^2}/(\mathrm{d}T/\mathrm{d}x_2)^2 M^2$ in time $\bar{\tau} = x/M$, in one of the above experiments the condition $(\vartheta^2)^\circ \ll (\overline{t^2})^\circ$ was realized under which the scalar field initially behaves as an isotropic one (see solution (16)). Further away the parameter θ approaches the asymptotic power 'law' (17). Within the range of the $\bar{\tau}$ values studied, there is an excellent agreement between the prediction and experiment. The situation is less satisfactory in Fig. 12 for the time scale $T_t = (\overline{t^2}/\varepsilon_t)U_\infty/M = (\sigma/6)R_c(\lambda_t/M)^2$, where $R_c = U_\infty M/\nu$, $\lambda_t^2 = 6\kappa\overline{t^2}/\varepsilon_t$, which probably can be ascribed to a not very accurate measurement of the scalar field 'dissipation' rate. It seems that the same reason is responsible for the fact that along with a good agreement between prediction and experiment for the lateral heat flux (Fig. 13), there is some discrepancy between the results compared for the par-

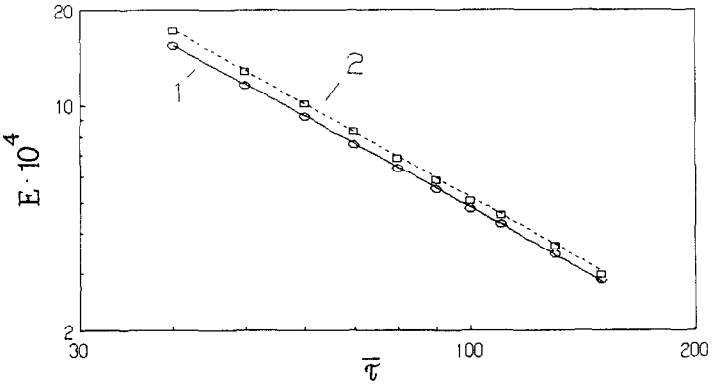

FIG. 9. Evolution of the kinetic energy of isotropic turbulence: ○, mandoline; □, toaster [9]; ——, numerical modelling.

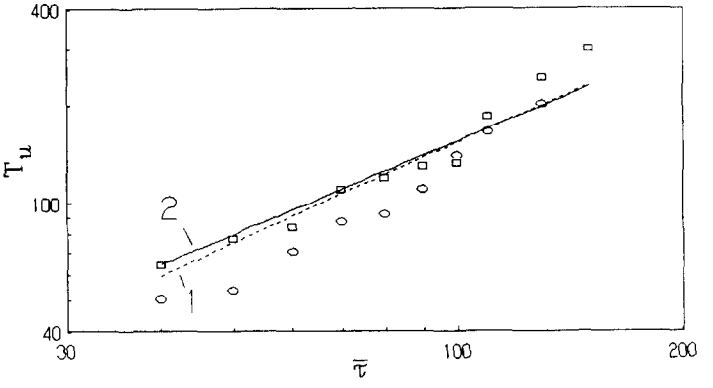

FIG. 10. Evolution of the time scale of velocity fluctuations. For notation see Fig. 9.

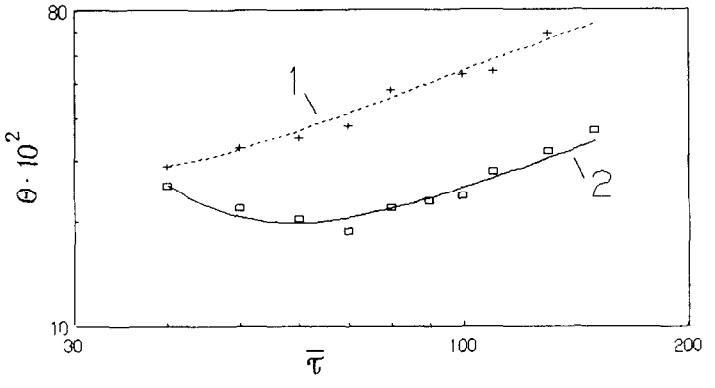

FIG. 11. Evolution of mean squared temperature fluctuations in the mandoline wake. Notation is that of ref. [9].

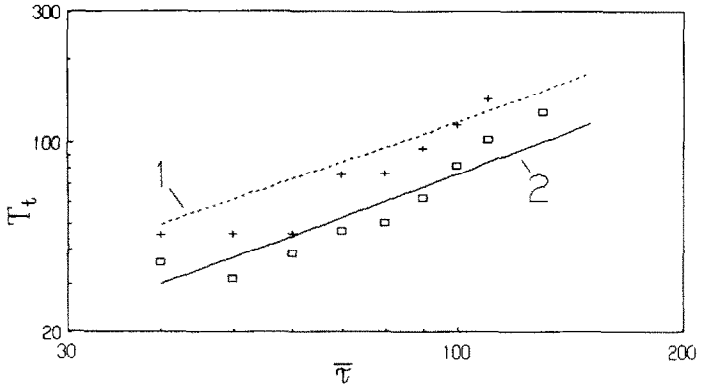

FIG. 12. Evolution of the time scale of temperature fluctuations. Notation is that of ref. [9].

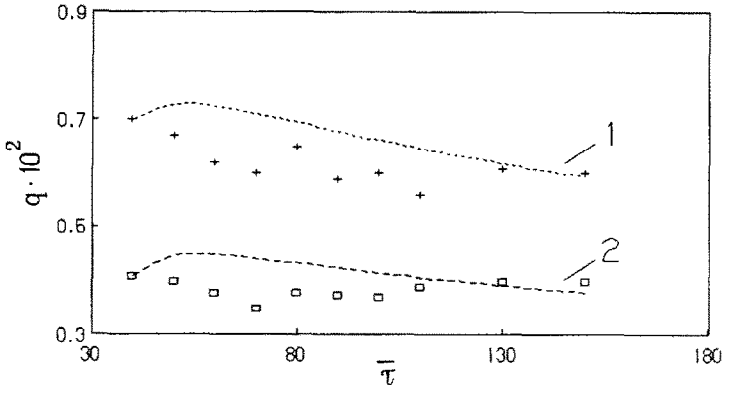

FIG. 13. Evolution of the transverse heat flux $q = -\overline{u_2 t}/U_x M \, dT/dx_2$ in the mandoline wake. Notation corresponds to that in ref. [9].

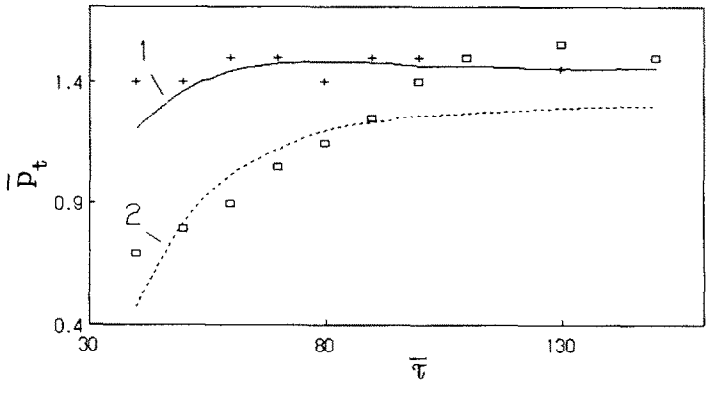

FIG. 14. Evolution of the ratio of the generation rate of temperature fluctuations to that of dissipation in the mandoline wake. Notation is that of ref. [9].

ameter $\bar{P}_t$ of the ratio between the rates of generation of the $\overline{t^2}$ parameter and of its dissipation (Fig. 14).

A 'pure' experiment (as regards the linearity of the mean temperature profile) is the experiment with another type of generator of temperature fluctuations—a 'toaster'. Comparison of numerical and experimental results presented in Figs. 15–18 reveals their more rigorous agreement in the initial region of scalar field development.

Both realizations considered ('mandoline' and

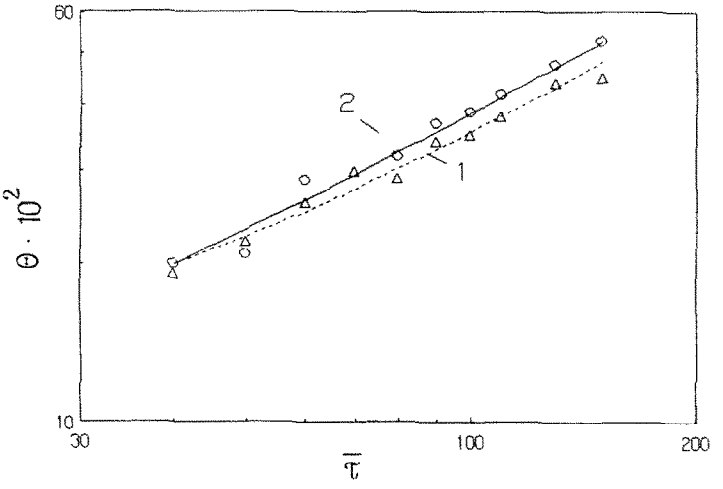

FIG. 15. Evolution of temperature fluctuations in the toaster wake. Notation is that of ref. [9].

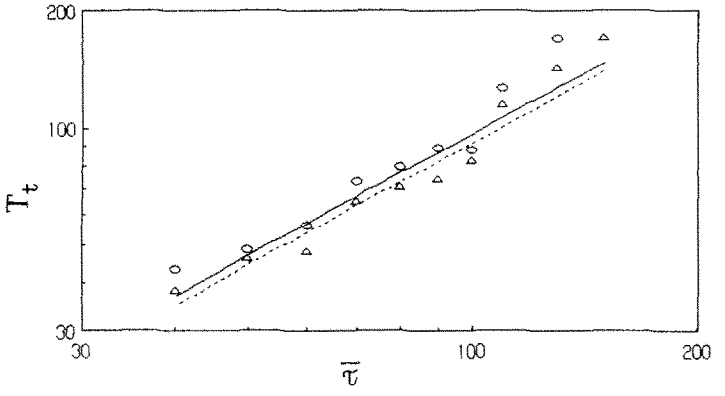

FIG. 16. Evolution of the time scale of temperature fluctuations in the toaster wake. Notation is that of ref. [9].

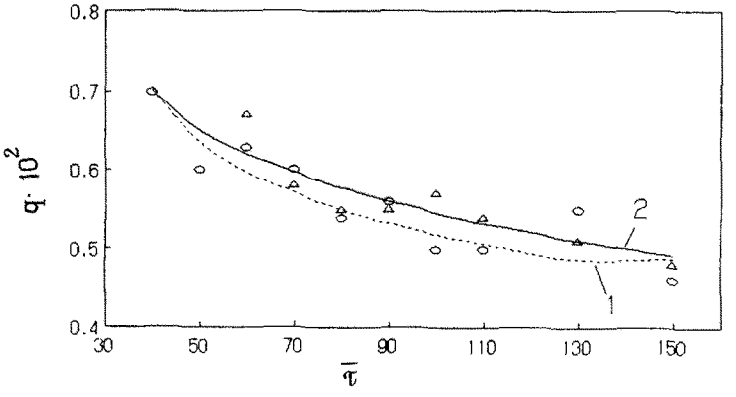

FIG. 17. Evolution of the transverse heat flux in the toaster wake [9].

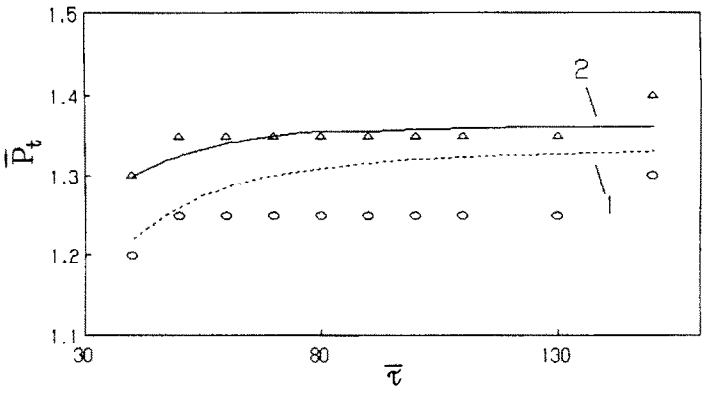

FIG. 18. Evolution of the parameter $\bar{P}_t$ in the toaster wake.

'toaster') were fulfilled at moderate turbulent Reynolds and Peclet numbers at which, however, the asymptotic solution for a strong turbulence (17)–(19) still could be satisfied as follows from the comparison of numerical and experimental data. At large values of the longitudinal coordinate (or at large evolution times), in view of the further decrease of R_λ and P_λ, the turbulence evolution should be substantially non-similar until inertia effects become so small that the scalar field turbulence dynamics regains its similarity which obeys the laws typical of the final stage of degeneration (20)–(22).

The transition to the final degeneration stage was investigated numerically by solving the problem at hand up to the evolution times at which asymptotics (20)–(22) are fulfilled. In what follows, the results of the Cauchy problem numerical solution under the initial conditions of ref. [9] for 'mandoline' at $dT/dx_2 = 7.48°C\ m^{-1}$ are presented.

The results of the numerical experiment given in Fig. 19 as the plots of E and T_u vs time show that the transition of the isotropic velocity field turbulence to the final degeneration stage occurs when $R_\lambda \simeq 0.25$. The evolution of the mean squared temperature fluctuations in Fig. 20 shows that as the turbulence energy decays the temperature fluctuations first increase (in accordance with the asymptotics of the strong scalar field turbulence (17)) and then, at sufficiently great evolution times (moderate values of R_λ and P_λ) the transition to the final stage takes place. At $\sigma \simeq 1$ this occurs at the same time values of $\bar{\tau}$ as does the final stage of velocity degeneration and is given by asymptotics (20). Presented in this figure are also the results of the numerical experiments for great and small molecular Prandtl numbers (recall that the second-order model (9)–(11) is universal with respect to this parameter). It can be easily seen that with $\sigma \gg 1$ the final stage sets in at larger values of $\bar{\tau}$ and with $\sigma \ll 1$

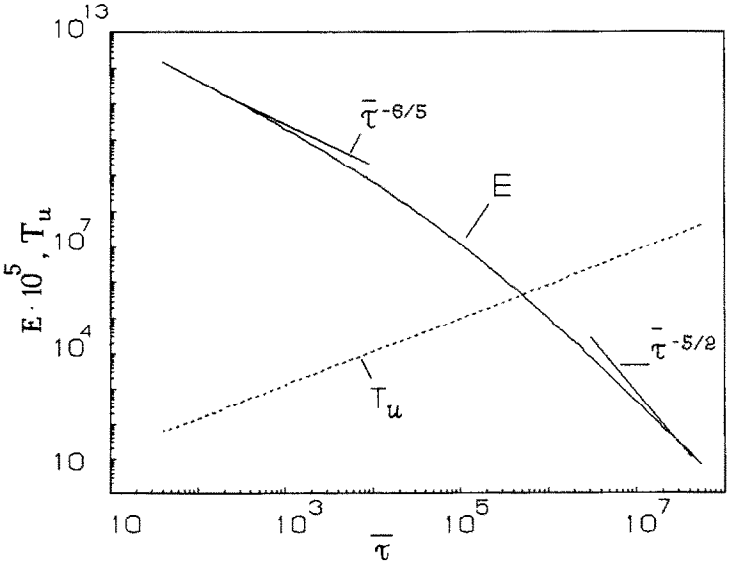

FIG. 19. Numerical modelling of the evolution of turbulence energy and of time scale up to the final stage of degeneration.

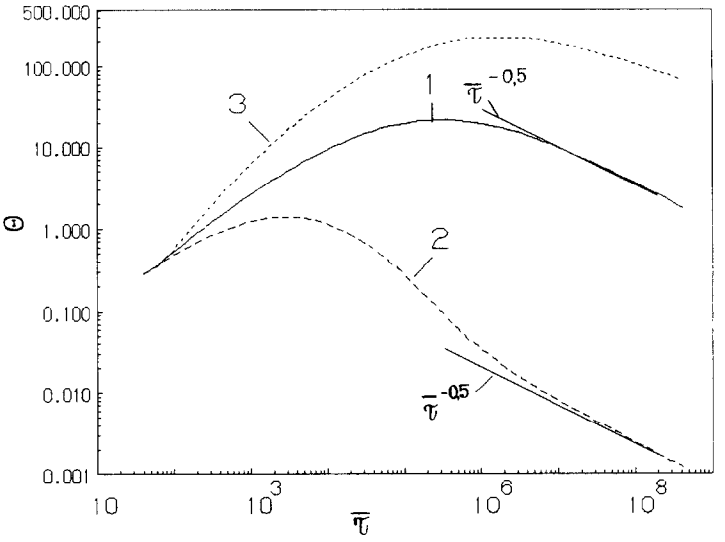

FIG. 20. Numerical modelling of the evolution of temperature fluctuations at $dt/dx_2 = \text{const.}$ in the isotropic velocity field up to the final stage of degeneration at different molecular Prandtl numbers: 1, $\sigma = 0.73$; 2, $\sigma = 10^{-2}$; 3, $\sigma = 10^3$.

at smaller values of $\bar{\tau}$ as against the case with $\sigma \simeq 1$.

The data given in Figs. 21–25 display the evolution (up to the final degeneration stage) of the remaining scalar field turbulence parameters: the time scale T_t (Fig. 21), the time scale ratio $R = T_u/T_t$ (Fig. 22), the lateral heat flux q (Fig. 23): the parameter $\tilde{P}_t$ representing the ratio of rates of the generation and 'dissipation' of temperature fluctuations (Fig. 24), and the correlation coefficient ρ_{2t}.

The above numerical experiment was undertaken to show, firstly, that the decaying isotropic velocity field at large evolution times drives the nearly homogeneous scalar field to the final stage which obeys the asymptotic solution of Dun and Reid [7]; secondly, that there is an effect of the molecular Prandtl number on the degeneration of a weak nearly homogeneous scalar field turbulence.

Note that as the turbulent Reynolds and Peclet numbers are interconnected

$$P_\lambda^2 = \frac{\lambda_t^2 \overline{q^2}}{\kappa^2} = \frac{6}{5}\sigma \frac{1}{R} R_\lambda^2$$

the scalar field 'inertia' (the parameter P_λ) depends, apart from R_λ, also on the parameters σ and R, i.e. at high values of R_λ the parameter P_λ can turn to be moderate or even small (at very small values of σ); conversely, at small values of R_λ the parameter P_λ can be rather large (at very high values of σ). Such a

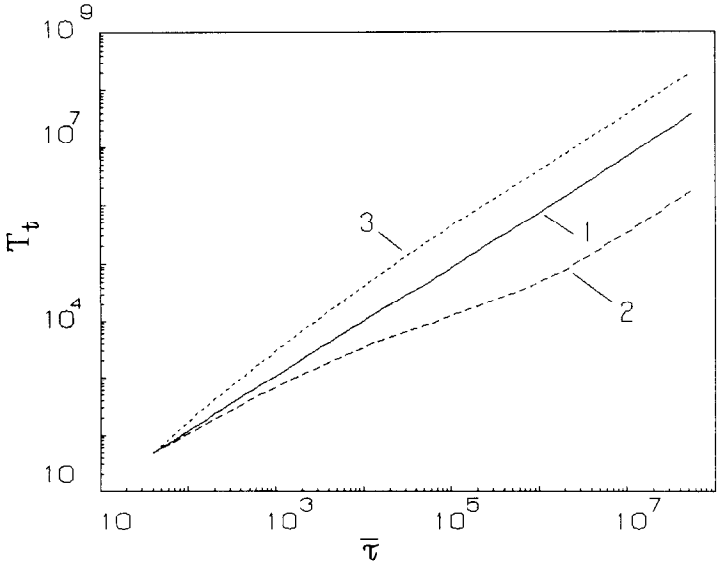

FIG. 21. Results of numerical modelling for the evolution of the time scale of temperature fluctuations.

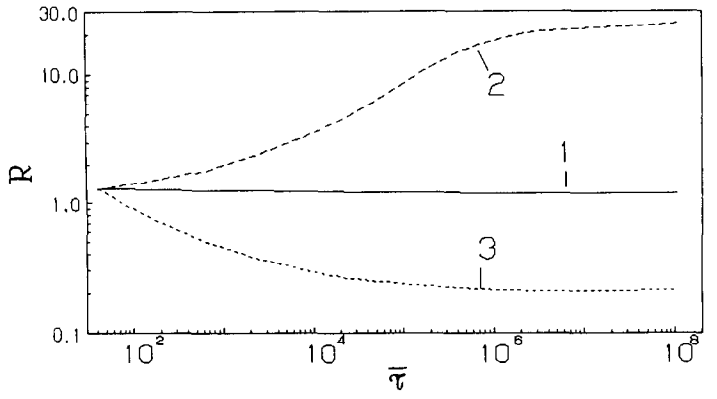

FIG. 22. Results of numerical modelling for the evolution of the ratio of time scales.

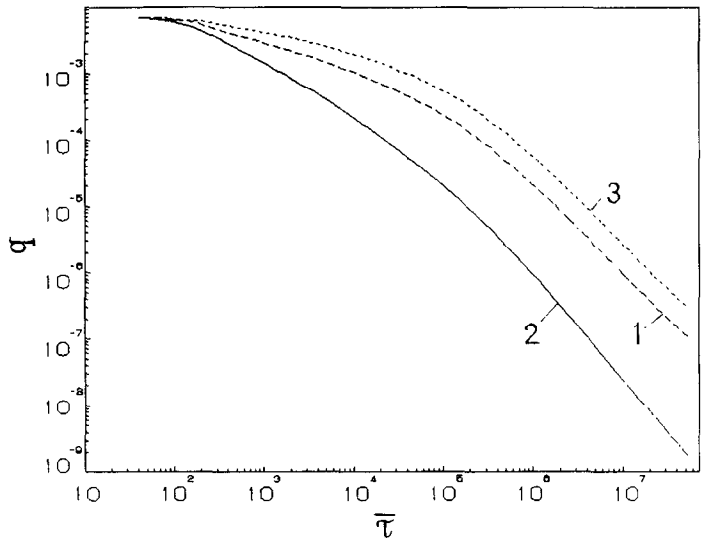

FIG. 23. Results of numerical modelling for the evolution of the transverse heat flux.

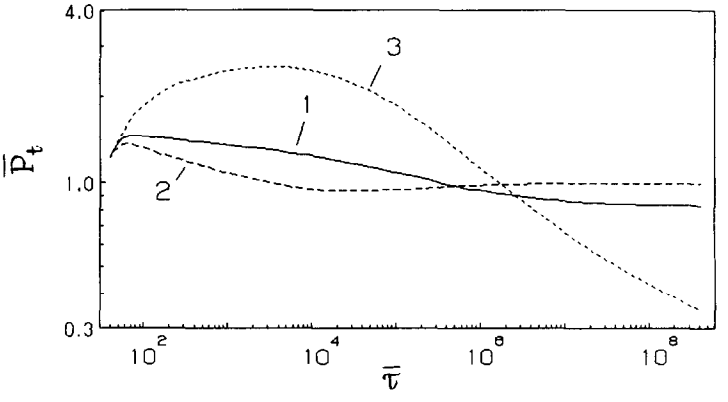

FIG. 24. Results of numerical modelling for the evolution of $\bar{P}_t$ parameter.

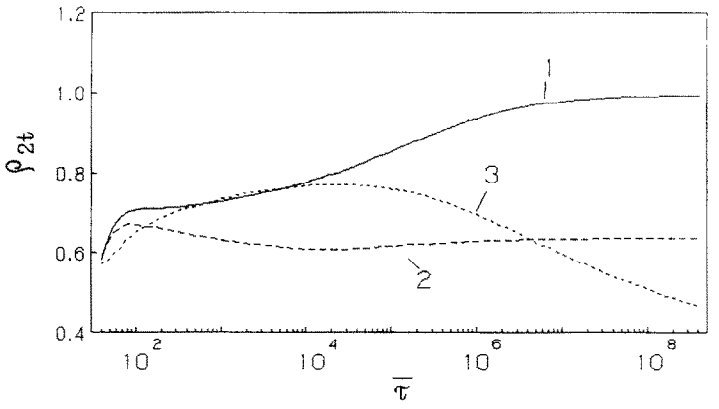

FIG. 25. Results of numerical modelling for the evolution of velocity–temperature correlation coefficient $\rho_{2t} = \overline{u_2 t}/(\overline{u_2^2})^{1/2}(\overline{t^2})^{1/2}$.

discrepancy between the inertia of the velocity and scalar fields may lead to a non-trivial degeneration of the scalar field, especially in the region of moderate values of R_λ, as is demonstrated in Figs. 20–25, namely a fast deviation of the scalar field parameters from the asymptotics of strong turbulence for $\sigma \ll 1$, an extension of the strong scalar field turbulence asymptotics to the region of moderate values of R_λ for $\sigma \gg 1$. This fact is of a fundamental importance for understanding the process of heat and mass transfer not only in the simplest constant gradient scalar field but in the case of substantially inhomogeneous turbulence of shear flows.

3.2. *The evolution of a nearly homogeneous scalar field in a nearly homogeneous velocity field*

The nearly homogeneous turbulence of the velocity and scalar fields is an approach to actual heat and mass transfer processes. The dynamics of such a velocity-scalar composition is described jointly by models (1), (2) and (9)–(11).

To qualitatively analyse the dynamics of a nearly homogeneous scalar field in an evolving nearly homogeneous velocity field, consider two limiting cases: $R_\lambda \gg 1$, $P_\lambda \gg 1$ and $R_\lambda \ll 1$, $P_\lambda \ll 1$.

In the case of a strong turbulence the velocity field is described by asymptotics (5) and (6). Using relations (13) and (14) in equation (10) for $\overline{t^2}$ it can be shown that its asymptotic (for $\bar{\tau} \gg 1$) solution has the form

$$\overline{t^2}_{\bar{\tau}\gg 1} = \frac{n_{ts}}{n_{us}} \frac{(\mathrm{d}T/\mathrm{d}x_2)^2}{(\mathrm{d}U_1/\mathrm{d}x_2)^2} \frac{(\mathscr{F}_{us}^{**}-2)}{R_\zeta^\circ} \times \frac{1}{(\mathscr{F}_{uw}^{**}-3+R_\zeta^\circ)} \overline{q^2}_{\bar{\tau}\gg 1}. \quad (23)$$

With this solution taken into account, the asymptotic relation for the parameter $\bar{P}_t$ can be given as

$$\bar{P}_{t_{/\tau\gg 1}} = 1 + (\mathscr{F}_{us}^{**}-3)/R_\zeta^\circ \quad (24)$$

analogously to relation (18). Then the asymptotic value of the correlation coefficient is attained

$$\rho_{2t}^2 = n_{ts}(\overline{q^2}/\overline{u_2^2})\bar{P}_t \quad (25)$$

where the asymptotic quantity $\overline{q^2}/\overline{u_2^2}$ is defined by relation (6).

In the case of a weak turbulence the velocity field is determined by asymptotic relations (7) and (8). It can be shown [1] that asymptotic relations for the scalar field have the form of relations (23)–(25) where the strong turbulence coefficients are replaced by those of weak turbulence: n_{us} by n_{uw}, n_{ts} by n_{ts}, F_{us}^{**} by F_{uw}^{**}, R_ζ° by $R_{\zeta w}$.

To check the validity of the asymptotic solutions and the adequacy of the model of arbitrary values of the parameters R_λ, P_λ, σ for $\bar{P}_u \neq 0$ and $\bar{P}_t \neq 0$, the Cauchy problem was solved numerically for the full system of equations (1), (2) and (9)–(11) under the initial conditions that correspond to the experiment of Tavoularis and Corrsin [4].

Figures 26–28 compare numerical and experimental data for the temperature field parameters

$$\Theta = \overline{t^2}\Big/\left(\frac{\mathrm{d}T}{\mathrm{d}x_2}\right)^2 h^2, \quad T_t = \frac{\overline{t^2}}{\varepsilon_t}\Big/\left(\frac{\mathrm{d}U_1}{\mathrm{d}x_2}\right), \quad R = T_u/T_t$$

$$q = -\overline{u_2 t}\Big/\frac{\mathrm{d}U_1}{\mathrm{d}x_2}\frac{\mathrm{d}T}{\mathrm{d}x_2}h^2, \quad \bar{P}_t = -\overline{u_2 t}\frac{\mathrm{d}T}{\mathrm{d}x_2}\Big/\varepsilon_t = qT_t/\Theta$$

where h is the lateral dimension of the region occupied by the flow. As follows from the plots, the model furnishes quite an adequate description of the experiment undertaken with a fairly strong turbulence ($R_\lambda \simeq 2\times 10^2$). Unfortunately, the range of $\bar{\tau}$ values in the experiment turned to be insufficient for the parameters to approach the asymptotics of a strong turbulence (as clearly displayed by the data of Figs. 26–28).

It has been already noted in Section 2 that in the case of initially strong nearly homogeneous turbulence the transition to the final stage is impossible. This is also true for a scalar nearly homogeneous field. To investigate the approach of the scalar field

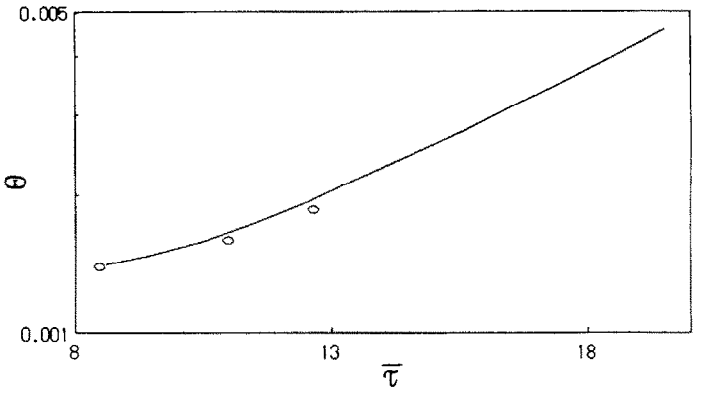

FIG. 26. Evolution of temperature fluctuations variance at $dT/dx_1 = \text{const.}$, $dU_1/dx_1 = \text{const.}$, $R_\lambda \gg 1$: ○, ref. [4]; ——, numerical modelling.

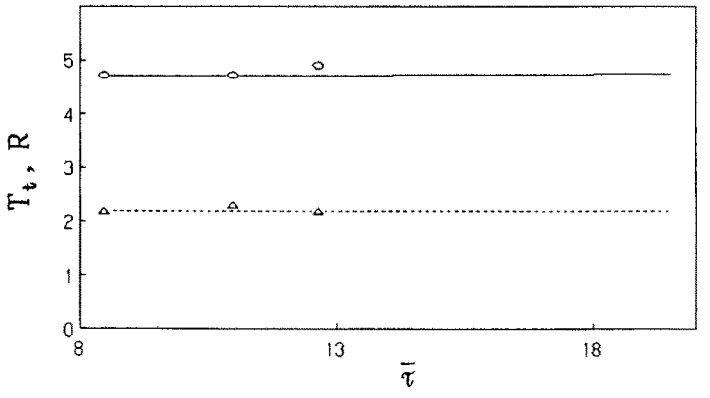

FIG. 27. Evolution of temperature fluctuations time scale, T_t, and of the time scale ratio, R: ○, T_t; △, R [4]; ——, numerical modelling.

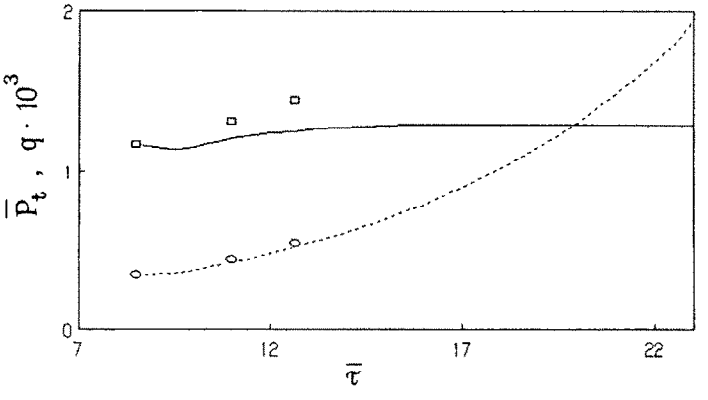

FIG. 28. Evolution of the transverse heat flux, q, and parameter $\bar{P}_t$: ○, q; □, $\bar{P}_t$; ——, numerical modelling.

parameters to the final stage asymptotics, a conventional numerical experiment was made to follow the development of a scalar field in the weak velocity field which was considered in Section 2 (Figs. 5–8). The results of this experiment for different molecular Prandtl numbers are presented in Figs. 29–32. From the plots given it follows that the analytical asymptotics of the final stage of a weak nearly homogeneous scalar field is fulfilled. The effect of molecular Prandtl number reveals in the extension, as compared with the case $\sigma \simeq 1$, of the final stage of $\sigma \gg 1$ and its relatively early occurrence for $\sigma \ll 1$. This effect can be explained physically: the processes of turbulent exchange enhance with a decrease in σ and diminish with an increase in σ. This is most clearly evidenced by the data for the turbulent Prandtl number in Fig. 32. It

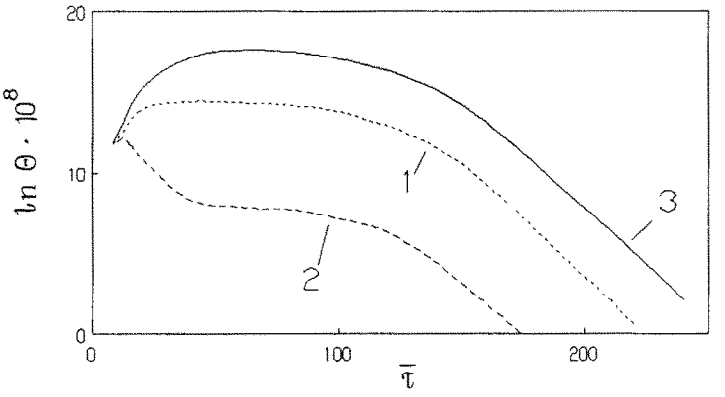

FIG. 29. Numerical modelling of the evolution of temperature fluctuations variance, Θ, at $dT/dx = \text{const.}$, $dU/dx_2 = \text{const.}$ and moderate values of R_i up to the final stage of degeneration: 1, $\sigma = 0.73$; 2, $\sigma = 10^{-2}$; 3, $\sigma = 10^3$.

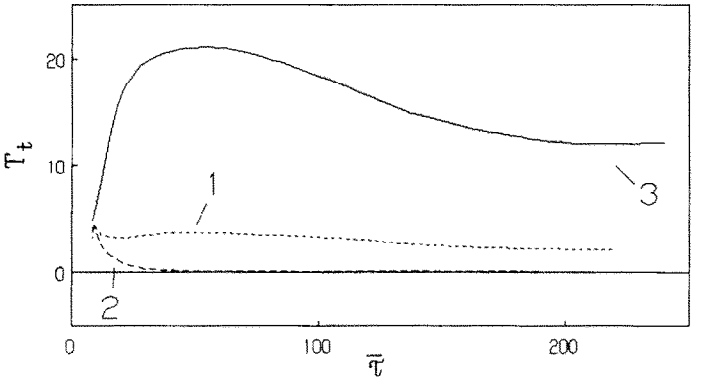

FIG. 30. Numerical modelling for the evolution of the time scale of temperature fluctuations: 1, $\sigma = 0.73$; 2, $\sigma = 10^{-2}$; 3, $\sigma = 10^3$.

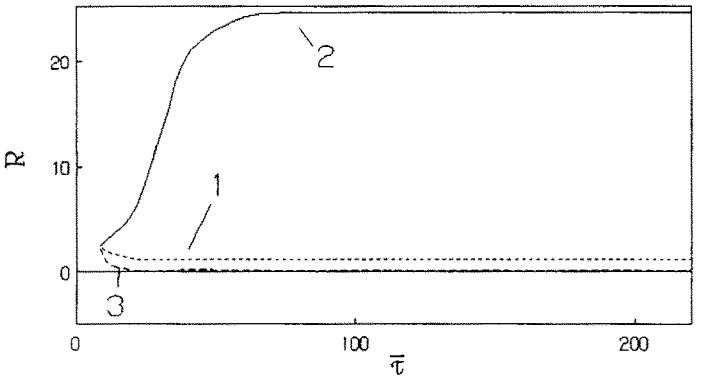

FIG. 31. Numerical modelling for the evolution of the time scale of ratio, R: 1, $\sigma = 0.73$; 2, $\sigma = 10^{-2}$; 3, $\sigma = 10^3$.

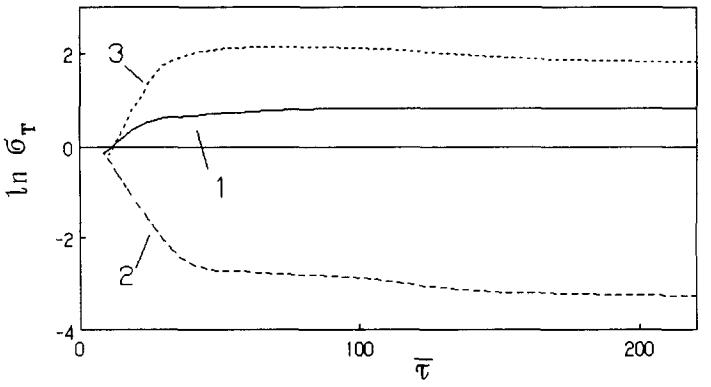

FIG. 32. Numerical modelling of the evolution of the turbulent Prandtl number: 1, $\sigma = 0.73$; 2, $\sigma = 10^{-2}$; 3, $\sigma = 10^{3}$.

should be noted that these data are in contradiction with the results of Deissler's spectral analysis [10] according to which with $\bar{\tau} \gg 1$ the parameter σ_T tends to unity irrespective of the magnitude of the molecular Prandtl number. The validity of the results obtained for the asymptotics $\bar{\tau} \gg 1$ could be judged from a direct numerical experiment concerned with modelling the evolution of a weak nearly homogeneous scalar field in a weak nearly homogeneous velocity field. Unfortunately, to the authors' knowledge, such data are not available.

4. CONCLUSIONS

The present work was aimed at the application of the earlier proposed [1] dynamic second-order model of the nearly homogeneous velocity and passive scalar field, which is universal with respect to the turbulent Reynolds and Peclet number and to the molecular Prandtl number, to the 'test' problems concerned with the evolution of the fields considered up to the final degeneration stage. The following problems have been considered:

(1) evolution of a strong turbulent velocity field generated by a constant, transverse to the flow, gradient of the mean velocity (nearly homogeneous turbulence);

(2) evolution of a nearly homogeneous turbulent velocity field up to the final stage of degeneration;

(3) evolution of a strong nearly homogeneous scalar field in a strong decaying homogeneous isotropic velocity field;

(4) evolution of a nearly homogeneous scalar field in a decaying homogeneous isotropic velocity field up to the final stage of degeneration;

(5) evolution of a nearly homogeneous scalar field in a strong nearly homogeneous velocity field;

(6) evolution of a nearly homogeneous velocity field in a weak nearly homogeneous velocity field up to the final stage of degeneration.

When possible, numerical results were compared with experimental data or with the results of analyses made by other authors. As the numerical results at moderate turbulent Reynolds and Peclet numbers and at arbitrary molecular Prandtl numbers are new, it is desirable that they were compared with the data of direct numerical simulation on the basis of three-dimensional non-stationary Navier–Stokes and transport equations. Unfortunately, such data are lacking at present.

Since the nearly homogeneous velocity and scalar fields represent, to a certain extent, the approach to the shear flow turbulence, the problems considered make it possible to analyse the dynamics of elementary events of turbulent transfer in actual turbulent incompressible fluid flows.

REFERENCES

1. B. A. Kolovandin and O. G. Martynenko, Heat/mass transfer in homogeneous turbulence, Keynote Lecture, 9th Int. Heat Transfer Conf., Jerusalem, pp. 415–420 (1990).
2. F. H. Champagne, Y. G. Harris and S. Corrsin, Experiments on nearly homogeneous turbulent shear flow, *J. Fluid Mech.* **41**(1), 81–139 (1970).
3. Y. G. Harris, J. A. H. Graham and S. Corrsin, Future experiments in nearly homogeneous turbulent shear flow, *J. Fluid Mech.* **81**(4), 657–687 (1977).
4. S. Tavoularis and S. Corrsin, Experiment in nearly homogeneous turbulent shear flow with a uniform mean temperature gradient, *J. Fluid Mech.* **104**(1), 311–347 (1981).
5. U. Karnik and S. Tavoularis, The asymptotic development of nearly homogeneous turbulent shear flow, *Proc. 4th Int. Symp. on Turbulent Shear Flows*, Karlsruhe, pp. 14.18–14.23 (1983).
6. R. Deissler, Effect of inhomogeneity and of shear flow in weak turbulent fields, *Physics Fluids* **4**(10), 1187–1198 (1961).
7. D. W. Dun and W. H. Reid, Heat transfer in isotropic turbulence during the final period of decay, NACA, TN 4186 (1958).

8. B. A. Kolovandin, N. N. Luchko and O. G. Martynenko, Modelling of homogeneous turbulent scalar dynamics, *Proc. 3rd Int. Symp. on Turbulent Shear Flows*, Davis, pp. 1017–1025 (1981).
9. A. Sirivat and Z. Warhaft, The effect of a passive cross-stream temperature gradient on the evolution of temperature variance and heat flux in grid turbulence, *J. Fluid Mech.* **128**, 323–346 (1983).
10. R. Deissler, Turbulent heat transfer and temperature fluctuation in a field with uniform velocity and temperature gradients, *Int. J. Heat Mass Transfer* **6**, 257–270 (1963).

MODELISATION DU DEVELOPPEMENT DES CHAMPS DE VITESSE ET DE SCALAIRE POUR LA TURBULENCE PRESQUE HOMOGENE

Résumé—On considère, à partir du modèle au second-ordre suggéré par Kolovandin et Martynenko (Heat/mass transfer in homogeneous turbulence, 9th Int. Heat Transfer Conf., Jerusalem (1990)), la modélisation numérique de la turbulence presque homogène des champs de vitesse et de scalaire passif transporté. On étudie en détail l'effet exercé par les facteurs principaux de la génération de la turbulence—les gradients des valeurs moyennes de vitesse et de scalaire—sur l'évolution dans le temps des caractéristiques statistiques de la turbulence qui, dans le cadre du modèle au second ordre, déterminent les mécanismes du transfert turbulent de quantité de mouvement et de chaleur pour des nombres quelconques de Reynolds et de Peclet.

MODELLIERUNG DER ENTWICKLUNG EINER NAHEZU HOMOGENEN TURBULENZ DER GESCHWINDIGKEITS- UND SKALARFELDER

Zusammenfassung—Auf der Grundlage des Modells zweiter Ordnung von Kolovandin und Martynenko (Heat/mass transfer in homogeneous turbulence, 9th Int. Heat Transfer Conf., Jerusalem (1990)) wird die nahezu homogene Turbulenz der Geschwindigkeits- und der transportierten passiven Skalar-Felder numerisch modelliert. Ziel der Arbeit ist eine detaillierte Untersuchung des grundlegenden Einflusses der Turbulenzerzeugung (die Gradienten der mittleren Geschwindigkeit und der skalaren Größen) auf die zeitliche Entwicklung des statistischen Turbulenzverhaltens. Diese bestimmen—innerhalb des Rahmens des Modells zweiter Ordnung—die Vorgänge beim turbulenten Impuls- und Wärmetransport bei beliebiger turbulenter Reynolds- und Peclet-Zahl.

МОДЕЛИРОВАНИЕ ОДНОРОДНОЙ ТУРБУЛЕНТНОСТИ СКАЛЯРНОГО ПОЛЯ

Аннотация—На основе предложенной в предыдущей работе [1] модели второго порядка рассматривается численное моделирование динамики обобщенно-однородной турбулентности полей скорости и переносимого пассивного скаляра. Работа направлена на детальное исследование влияния основных факторов генерирования турбулентности—градиентов осредненных значений скорости и скаляра на эволюцию во времени статистических характеристик турбулентности, определяющих в рамках модели второго порядка процессы турбулентного переноса импульса и тепла или массы при произвольных значениях турбулентных чисел Рейнольдса и Пекле и молекулярного числа Прандтля.